J. Plasma Phys. (2024), *vol*. 90, 905900611
Published by Cambridge University Press

doi:10.1017/S0022377824000941

Outside and inside a magnetic island: different perspectives to describe the same observables

B. Momo [1] **and I. Predebon** [1,2,†]

[1]Consorzio RFX (CNR, ENEA, INFN, Università di Padova, Acciaierie Venete SpA), corso Stati Uniti 4, I-35127 Padova, Italy

[2]Istituto per la Scienza e Tecnologia dei Plasmi - CNR, corso Stati Uniti 4, I-35127 Padova, Italy

(Received 24 April 2024; revised 15 July 2024; accepted 24 July 2024)

We compare three different approaches to describe a magnetic island in a generic toroidal plasma: (i) perturbative, from the perspective of the equilibrium magnetic field and the related action in a variational principle formulation; (ii) again perturbative, based on the integrability of a system with a single resonant mode and the application of a canonical transformation onto a new island equilibrium system; and (iii) non-perturbative, making use of a full geometric description of the island considered as a stand-alone plasma domain. For the three approaches, we characterize some observables and discuss the respective limits.

Key words: plasma instabilities, plasma nonlinear phenomena, fusion plasma

1. Introduction

The tearing instability, growing near the rational surfaces, leads to helical magnetic perturbations that can change the magnetic topology, with the formation of magnetic islands through a reconnection process in which the field lines break and reconnect. Especially for the description of magnetic field line trajectories, it is convenient to express the magnetic field in terms of its vector potential. In this way, the magnetic field line equations can be derived from a variational principle, formally identical to the action principle in phase space with a Hamiltonian H (Cary & Littlejohn 1983; Elsasser 1986; Hazeltine & Meiss 1992). The magnetic field line equations are the paths that extremize the action S_γ, and are formally identical to the canonical equations of motion in phase space. The identification of canonical and magnetic variables follows the paper by Pina & Ortiz (1988): the symmetry coordinate (e.g. the toroidal angle φ in an axisymmetric magnetic field) is identified with the time t, another space coordinate (the poloidal angle ϑ) plays the role of the canonical position q, whereas the poloidal and toroidal magnetic fluxes, ψ_p and ψ_t, have their equivalence in the Hamiltonian H and canonical momentum p, respectively (when the symmetry coordinate is the toroidal one). Hidden in these identifications is the additional equivalence between the covariant components A_i of the vector potential and

† Email address for correspondence: italo.predebon@istp.cnr.it

the magnetic fields, which follows from Stokes theorem. A pedagogical presentation of the above elements is available in the recent review paper by Escande & Momo (2024).

Following the Hamiltonian formulation of the magnetic field line equations, in this work, we compare three different methods to characterize a magnetic island in terms of some observables (e.g. the island width or its volume) which cannot depend on a particular coordinate system, vector potential gauge or choice of perturbative/non-perturbative approach. The first two methods consider the island as a single-mode perturbation of the equilibrium Hamiltonian and provide a description of the observables, say, from outside the island; conversely, the other method considers the island as a stand-alone plasma subdomain with a self-consistent representation of the observables from its inside.

With the first perturbative approach, we consider an (m, n) tearing mode (where m and n are the poloidal and the toroidal mode number, respectively) at the resonant surface where the island opens, defined by the rational value $\iota = n/m$ of the rotational transform profile. We apply a new formulation for the island width based on the definition of the action S_γ of the magnetic system that returns the same result as the island width estimated from the amplitude of the cat's eye pendulum Hamiltonian in phase space (Escande & Momo 2024). The width classically depends on a flux Φ related to the radial magnetic perturbation at the rational surface (Park, Boozer & Menard 2008; White 2013). Escande & Momo (2024) identified this flux – with a clear geometrical meaning and independently of the coordinate system – as the flux through the ribbon enclosed by the orbits of the O-point and the X-point of the island. In this work, we extend its validity even to non-perturbative contexts, showing that it can be interpreted as the helical flux through the island separatrix independently of the approach adopted.

In the second method, we exploit the integrability of the Hamiltonian of a perturbed system that preserves the helical symmetry, defining the island domain as a new equilibrium with its own magnetic axis corresponding to the O-point of the island. Magnetic coordinates are defined on the island flux surfaces as canonical action-angle coordinates, providing a definition of magnetic fluxes through the island flux surfaces, as well as other quantities like the island volume and width (Martines *et al.* 2011; Momo *et al.* 2011). The transition from a perturbed Hamiltonian to a new equilibrium Hamiltonian represents the change of perspective claimed in the title of the paper, moving from the view of an axisymmetric equilibrium with an external magnetic axis with respect to the island (perspective from outside the island) to the island domain itself with its own action-angle coordinates (perspective from inside the island).

In the third, non-perturbative approach, the island domain is considered independently of the surrounding plasma. It is geometrically characterized in terms of magnetic coordinates and metric tensor starting from a discretized field map, again providing integral quantities like the magnetic fluxes, the island volume and width, which are, in principle, measurable (Predebon *et al.* 2018).

The three methods are compared for the calculation of several observables of two experimental islands, (1, 1) for a circular tokamak and (1, 7) for a reversed-field pinch (RFP) plasma. The agreement is satisfactory. In particular, the comparison of the island width provides a first validation of the formula introduced by Escande & Momo (2024) in a perturbative context and shows the validity of the new interpretation of the flux Φ (hereafter Φ_{OX}) as the helical flux through the island separatrix, particularly relevant when the island is characterized in non-perturbative contexts.

The paper is structured as follows: the two perturbative approaches are introduced in §§ 2 and 3, and the non-perturbative approach in § 4; in the following § 5, we compare the three methods for a (1, 1) tokamak island and a (1, 7) RFP island in a toroidal device with circular cross-section, with a brief summary closing the paper.

https://doi.org/10.1017/S0022377824000941 Published online by Cambridge University Press

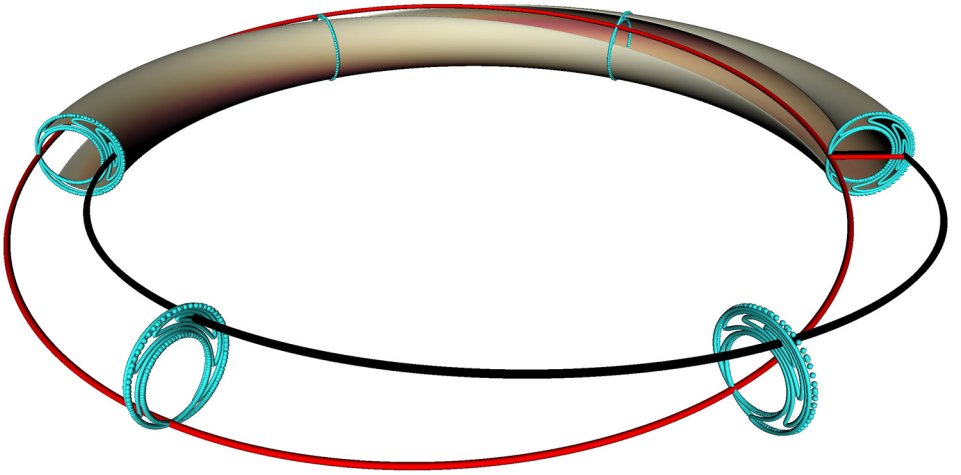

FIGURE 1. Helical ribbon defining the Φ_{OX} flux for a (1, 1) magnetic island, with the closed orbits corresponding to the O- and the X-point in black and red, respectively.

2. Magnetic islands in a perturbative approach

Magnetic islands are due to non-vanishing resonant magnetic perturbations in the plasma, and a perturbative approach is therefore frequently used for their description. In particular, a magnetic island with poloidal m and toroidal n periodicity opens around the resonant flux surface defined by the rational value $\iota = n/m$ of the rotational transform related to the unperturbed equilibrium configuration.

The island width is commonly computed in terms of the geometric width of a pendulum-like cat's eye in the context of small resonant perturbations of a regular magnetic field, associated with a time-independent Hamiltonian (Hazeltine & Meiss 1992; White 2013). In all cases, the width of a magnetic island is proportional to the square root of a magnetic flux, which turns out to be the perturbation of a helical flux evaluated on the resonant flux surface (Park *et al.* 2008; Predebon *et al.* 2016). As shown in § 3, this flux can be interpreted as the helical flux through the separatrix.

In this section, we exploit the existence of a coordinate-independent magnetic flux related to a magnetic island that correctly estimates its width, as proved by Escande & Momo (2024): this flux, named Φ_{OX}, is defined for each magnetic island through the ribbon defined by the periodic orbits related to the O- and X-points shown in figure 1. The above path is based on the variational principle formulation for magnetic field lines and on the related action

$$S_\gamma = \int_\gamma \boldsymbol{A}(\boldsymbol{x}) \cdot \mathrm{d}\boldsymbol{x}, \tag{2.1}$$

where $\boldsymbol{x}$ is the spatial coordinates vector, $\boldsymbol{A}$ is the vector potential, $\boldsymbol{B} = \boldsymbol{\nabla} \times \boldsymbol{A}$ and the integral runs along the path γ between two points of a magnetic field line. When γ is a closed circuit, the Stokes theorem states that the action S_γ is the magnetic flux through the surface having this circuit as a boundary.

To relate the action S_γ to the resonant perturbation that opens an island, the formal identification between canonical and magnetic coordinates, and the equivalence between the covariant components A_i, $i = 1, 2, 3$ (where the index i corresponds e.g. to the radial, poloidal and toroidal coordinate, respectively) of the vector potential and the magnetic fluxes must be used in the definition of S_γ. This equivalence is only valid in the axial

https://doi.org/10.1017/S0022377824000941 Published online by Cambridge University Press

gauge $A_1 = 0$,

$$\begin{aligned} S_\gamma &= \int_\gamma (A_2\,\mathrm{d}x^2 + A_3\,\mathrm{d}x^3) \\ &= \frac{1}{2\pi}\int_\gamma (p\,\mathrm{d}\vartheta - H\,\mathrm{d}\varphi) \\ &= \frac{1}{2\pi}\int_\gamma (\psi_t\,\mathrm{d}\vartheta - \psi_p\,\mathrm{d}\varphi), \end{aligned} \tag{2.2}$$

with $x^2 = \vartheta$ and $x^3 = \varphi$ poloidal and toroidal angles; the relations $p = \psi_t$ and $H = \psi_p$ define the identifications between the canonical momentum and the toroidal magnetic flux, and between the Hamiltonian and the poloidal flux, respectively, assuming the canonical position and time to be $q = x^2 = \vartheta$ and $t = x^3 = \varphi$.

Figure 1 visualizes the helical ribbon defined by the orbits of the O- and X-points, and helps understand the geometrical meaning of the flux Φ_{OX} through that ribbon. Using the definition of the action for a magnetic field line, the Φ_{OX} flux turns out to be $S_O - S_X$, where S_O is the action computed along the closed orbit defined by the O-point, and S_X the action along the closed orbit defined by the X-point. In the rest of this section, we revisit the derivation of § 5 of the review by Escande & Momo (2024) writing the island width as a function of Φ_{OX}.

Let $\boldsymbol{x} = (\psi_t^0, \vartheta, \varphi)$ be magnetic coordinates for the unperturbed equilibrium. If the perturbation is not large enough to violate the requirement of a non-null Jacobian, then the full perturbed system around the resonant surface, in the same $\boldsymbol{x}$ coordinate system, is approximated by

$$\psi_t(\boldsymbol{x}) \simeq \psi_t^0 + \psi_t^{m,n}(\psi_t^0)\,\mathrm{e}^{\mathrm{i}u} + \text{c.c.}, \tag{2.3}$$

$$\psi_p(\boldsymbol{x}) \simeq \psi_p^0 + \psi_p^{m,n}(\psi_t^0)\,\mathrm{e}^{\mathrm{i}u} + \text{c.c.}, \tag{2.4}$$

where $u = m\vartheta - n\varphi$ is called helical angle and c.c. indicates the complex conjugation. The unperturbed flux, $\psi_p^0 = \psi_p^0(\psi_t^0)$, defines the unperturbed equilibrium and its flux surfaces through the relation $\iota = \mathrm{d}\psi_p^0/\mathrm{d}\psi_t^0 = \mathrm{d}\vartheta/\mathrm{d}\varphi$. The $\psi^{m,n}(\psi_t^0) = |\psi^{m,n}|\,\mathrm{e}^{\mathrm{i}\alpha^{m,n}}$ terms are the Fourier components of the fluxes having the resonant periodicity.

We now better define the actions S_O and S_X, which are the line integrals along the lines defined by the O- and X-point of the (m, n) magnetic island, respectively. In calculating S_O and S_X from (2.2) using definitions (2.3) and (2.4), we assume that m and n are mutually relatively prime; φ varies by $2\pi m$ along O or X and ϑ varies by $2\pi n$, while the helical angles along the O and X orbits (u_O and u_X, respectively) are constant.

We first compute the action S_O:

$$\begin{aligned} S_O &= \frac{1}{2\pi}\int_O (\psi_t \mathrm{d}\vartheta - \psi_p \mathrm{d}\varphi) \\ &= (n\psi_t^0 - m\psi_p^0)|_{res} + (n\psi_t^{m,n} - m\psi_p^{m,n})|_{res}\,\mathrm{e}^{\mathrm{i}u_O} + \text{c.c.}, \end{aligned} \tag{2.5}$$

where all radial functions must be evaluated on the rational surface defined by $\iota = n/m$, even if not explicitly stated in the following notation. Introducing the helical flux function

$$\psi_h(\psi_t^0, u) = m\psi_p - n\psi_t, \tag{2.6}$$

https://doi.org/10.1017/S0022377824000941 Published online by Cambridge University Press

S_O can be written in terms of this flux through the O-point orbit as

$$\begin{aligned} -S_O &= \psi_h(\psi_t^0, u_O) \\ &= \psi_h^0 + |\psi_h^{m,n}|\, \mathrm{e}^{\mathrm{i}(u_O+\alpha_h^{m,n})} + \text{c.c.}, \end{aligned} \tag{2.7}$$

where $\psi_h^0 = \psi_h^0(\psi_t^0)$ is the unperturbed equilibrium flux, whereas $|\psi_h^{m,n}|$ and $\alpha_h^{m,n}$ are the amplitude and phase of the (m, n) Fourier component.

The calculation of the S_X flux follows the same steps, with u_O being substituted by u_X, and remembering that u_X is shifted by π with respect to u_O: $u_O + \alpha_h^{m,n} = 0, \pi$ and $u_X + \alpha_h^{m,n} = \pi, 0$, depending on the sign of the magnetic shear. This yields

$$\begin{aligned} -S_O(\psi_t^0) &= \psi_h^0 + 2|\psi_h^{m,n}| \cos(u_O + \alpha_h^{m,n}) \\ &= \psi_h^0 \pm 2|\psi_h^{m,n}|, \end{aligned} \tag{2.8}$$

$$\begin{aligned} -S_X(\psi_t^0) &= \psi_h^0 + 2|\psi_h^{m,n}| \cos(u_X + \alpha_h^{m,n}) \\ &= \psi_h^0 \mp 2|\psi_h^{m,n}|, \end{aligned} \tag{2.9}$$

$$\Phi_{OX} \equiv S_O - S_X = \mp 4|\psi_h^{m,n}|, \tag{2.10}$$

with all radial functions evaluated on the rational surface. The minus sign in (2.10) corresponds to a negative magnetic shear at the rational surface ($\mathrm{d}\iota/\mathrm{d}\psi_t^0 < 0$), which implies $u_O + \alpha_h^{m,n} = 0$, while the positive sign corresponds to the opposite case ($\mathrm{d}\iota/\mathrm{d}\psi_t^0 > 0$), with $u_O + \alpha_h^{m,n} = \pi$.

From an operative point of view, the Φ_{OX} flux can be computed both from (2.10) or by solving numerically the line integrals in (2.2) for $\gamma = O$ and $\gamma = X$. In the first case, one needs to evaluate the helical flux perturbation at the resonant surface; in the second case, one needs to know the path of the island extrema.

The amplitude of the magnetic island can then be computed from the formula (similar to (90) of Escande & Momo 2024)

$$W_{\Phi_{OX}} = 4\sqrt{\left|\frac{\Phi_{OX}}{2m\dfrac{\mathrm{d}\iota}{\mathrm{d}\psi_t^0}}\right|}\left(\frac{\mathrm{d}r}{\mathrm{d}\psi_t^0}\right), \tag{2.11}$$

where the factor $(\mathrm{d}\psi_t^0/\mathrm{d}r)^{-1}$ brings the width in units of a length. It implies a clear relation between the unperturbed flux ψ_t^0 and a radial coordinate r in meters: when r is the radius of the circular flux surface's cross-section of the zeroth-order equilibrium, the factor $(\mathrm{d}\psi_t^0/\mathrm{d}r)^{-1}$ considers the same amplitude at any poloidal or toroidal cuts. All radial functions, as the magnetic shear or the $(\mathrm{d}\psi_t^0/\mathrm{d}r)^{-1}$ term, must be evaluated at the resonant surfaces.

3. Magnetic islands as new equilibrium systems

In § 2, we stated the equivalence between the magnetic action along a helical path γ and the helical flux. From this perspective, (2.8) and (2.9) can be written in a shorter notation:

$$-S_O = \psi_h|_O, \tag{3.1}$$

$$-S_X = \psi_h|_X, \tag{3.2}$$

https://doi.org/10.1017/S0022377824000941 Published online by Cambridge University Press

and therefore,

$$\Phi_{OX} \equiv S_O - S_X = -\psi_h|_O + \psi_h|_X, \tag{3.3}$$

where $\psi_h|_O$ means the helical flux evaluated along the line defined by the O-point, and similarly $\psi_h|_X$. From a geometrical point of view, S_O can be interpreted as the helical flux $\psi_h|_O$ through the the surface delimited by the orbit of the centre of the island (O-point), and S_X as the helical flux $\psi_h|_X$ through the edge of the island (the orbit defined by the X-point). In this section, as well as in § 4, a way to compute the magnetic fluxes through any island flux surface is shown.

The perturbative approach in § 2 assumes an integrable unperturbed magnetic field configuration, i.e. the equation of motion can be solved to give non-chaotic magnetic field lines and therefore conserved magnetic flux surfaces. In the presence of general magnetic perturbations, the system is not integrable and flux surfaces are destroyed. Apart from an axisymmentric system, there is only one other known integrable system, i.e. that of helical symmetry, that defines conserved magnetic flux surfaces, analogous to the constant energy surfaces. In both cases, the Hamiltonian is time-independent and the equivalence $t = \varphi$ holds.

Equations (2.3) and (2.4), adding to the unperturbed equilibrium a single Fourier perturbation, define a helical integrable Hamiltonian. To integrate it, we make use of the change of coordinates $(\psi_t^0, \vartheta, \varphi) \mapsto (\psi_t^0, u, \varphi)$, where $u = m\vartheta - n\varphi$ is the helical variable. This change of coordinates defines a new time-independent Hamiltonian: the helical flux $\psi_h(\psi_t^0, u) = m\psi_p - n\psi_t$, which can be assumed as a radial variable of any system with a helical symmetry (Hazeltine & Meiss 1992). In fact, in the new coordinates, the identifications with the (p, q, t) variables are $q = x^2 = u, t = x^3 = \varphi$ and therefore $p = \psi_t, H = \psi_h$.

The island domain can be modelled as a helical equilibrium configuration, and a reconstruction of such equilibria has been implemented in a code named SHEq (Martines *et al.* 2011), now extended to the tokamak case too. The method is based on the superposition of an axisymmetric equilibrium and of a first-order helical perturbation computed according to Newcomb's equation supplemented with edge magnetic field measurements (Zanca & Terranova 2004); more details are in § 5. The helical flux contours give the shape of the flux surfaces of a helical domain. An example of such surfaces is shown in figure 2 (bottom half of panel *a*) for a magnetic island in an RFP plasma. The accuracy of the flux surface reconstruction is confirmed by the corresponding discretized field map (top half of panel *a*) obtained with the field line tracing code Flit, which integrates the field lines with the same helical Fourier perturbations (Innocente *et al.* 2017). The value of helical flux through the surfaces delimited by the X- and O-point orbits (their intersection with the poloidal plane respectively plotted in the figure with an orange and green dot) can be identified from the value of the helical flux at the extrema of its profile on the equatorial plane (figure 2*b*). The values of the helical flux above the value at the separatrix (orange dashed line in figure 2*b*) label the external flux surfaces with respect to the magnetic island, so the helical flux profile computed by the SHEq code is here cut at the separatrix to restrict the computation to the island domain. The values of ψ_h in the well between the X- and the O-point correspond to the island flux surfaces; whereas the values of ψ_h in the other well correspond to the circular flux surfaces around the axisymmetric equilibrium axis. It is worth noting that the evaluation of the helical flux on the X- and O-points enables an evaluation of the Φ_{OX} flux from (3.3) and, therefore, the island width from (2.11).

We can now define a new reference frame having its axis on the O-point of the island. From here on, we introduce the new index $\cdot_H$ to explicitly identify the quantities

https://doi.org/10.1017/S0022377824000941 Published online by Cambridge University Press

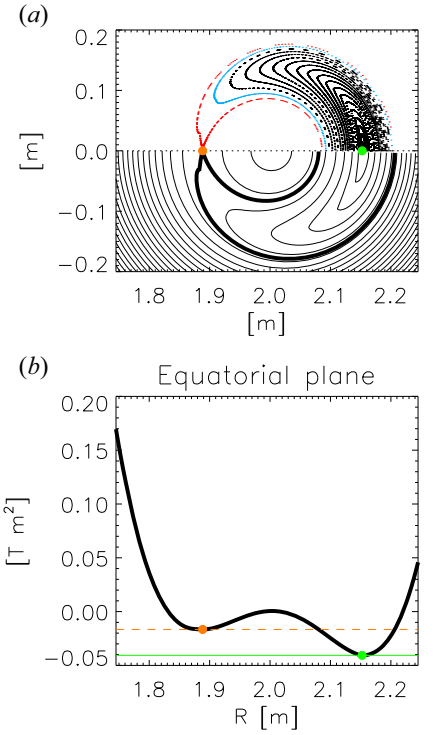

FIGURE 2. (*a*) $\varphi = 0$ discretized field map of a $(1, 7)$ island (top half of the section) and corresponding flux surface contour (bottom half) in a circular RFP. Red and light-blue curves in the top half-panel represent the two last flux surfaces from the Flit code (Innocente *et al.* 2017), the thick line in the bottom half-panel the separatrix computed by the Sheq code (Martines *et al.* 2011), and coloured dots the *X*- (orange) and *O*-points (green). (*b*) Helical flux ψ_h on the equatorial plane passing through the *X*- (orange) and *O*-points (green).

related to the helical magnetic flux surfaces Σ_H from the *O*-point to the separatrix. A time-independent canonical change of coordinates allows us to write the Hamiltonian of the helical system, ψ_h, in its action-angle form, ψ_H, where both the poloidal and toroidal fluxes across the helical flux surfaces are constants of the motion (Momo *et al.* 2011) and therefore functions of ψ_H. Due to the time independence of the canonical transformation, ψ_h and ψ_H define the same flux surfaces. Using the definition of the canonical action coordinate, the identifications between canonical and magnetic coordinates, and the perturbed fluxes in (2.3) and (2.4), the toroidal flux through Σ_H is defined by

$$\psi_{Ht}(\psi_H) = \frac{1}{2\pi} \oint p(E, q)\, \mathrm{d}q = I(E) \tag{3.4}$$

$$= \frac{1}{2\pi} \oint_{\Sigma_H} \psi_t(\psi_h, u)\, \mathrm{d}u. \tag{3.5}$$

Equation (3.4) is the standard formula for the canonical action coordinate, usually indicated with the symbol $I(E)$ for a given energy value E, and q the canonical position (Arnol'd 2013). In (3.5), the identifications with canonical coordinates have been used, the constant energy value E corresponds to the constant value of ψ_h on Σ_H and the expression (2.6) for the helical flux has been inverted to obtain $\psi_t(\psi_h, u)$. It is worth noting that on

https://doi.org/10.1017/S0022377824000941 Published online by Cambridge University Press

the right-hand side of this equation, the perturbed quantities appear, as ψ_t and ψ_h, while on the left-hand side, we have the quantities through the island flux surfaces, identified by $\cdot_H$. As a side remark, the action coordinate in (3.4) is not related to the magnetic action in (2.1). The angle coordinate, defined on the helical axis, is defined by (Arnol'd 2013)

$$u_H = \int_{q_0}^{q} \frac{\partial p(I, q')}{\partial I}\, \mathrm{d}q' \tag{3.6}$$

$$= \int_{0}^{u} \frac{\partial \psi_t(\psi_H, u')}{\partial \psi_{Ht}}\, \mathrm{d}u', \tag{3.7}$$

which turns out to be the straight-helical-like angle defined on the helical axis (the O-point of the island) which increases by 2π one turn around every helical flux surface.

Equation (3.5) implies that both magnetic fluxes (the action ψ_{Ht} and the Hamiltonian ψ_H of the system) are constant of the motion, i.e. are constant on magnetic flux surfaces. Moreover, magnetic field lines written in the action-angle coordinates are straight lines in the (u_H, φ) plane. The definitions of a helical angle and of a helical flux,

$$u_H = m\vartheta_H - n\varphi, \tag{3.8}$$

$$\psi_H = m\psi_{Hp} - n\psi_{Ht}, \tag{3.9}$$

bring to the definition of the new poloidal-like angle ϑ_H defined on the island O point and, implicitly, of the poloidal flux through Σ_H, $\psi_{Hp} = (\psi_H + n\psi_{Ht})/m$. The rotational transform related to straight-field-lines in the plane (ϑ_H, φ) is defined by

$$\iota_H = \frac{\mathrm{d}\vartheta_H}{\mathrm{d}\varphi} = \frac{\mathrm{d}\psi_{Hp}}{\mathrm{d}\psi_{Ht}}, \tag{3.10}$$

which counts the poloidal and toroidal turns of an island magnetic field line seen by an external observer. Moreover, the Jacobian and the metric elements of the $(\psi_H, \vartheta_H, \varphi)$ coordinate system allow us to calculate any geometric quantity related to the island domain, as the island volume, using the procedure that will be described in the next section for the stand-alone coordinate system.

We remark that the helical fluxes, $\psi_h(\psi_t^0, u)$ and $\psi_H(\psi_{Ht})$ in (2.6) and (3.9), respectively, are the same flux, due to the fact that the coordinate transformation $(\psi_t^0, u, \varphi) \mapsto (\psi_H, \vartheta_H, \varphi)$ is equivalent to a time-independent canonical transformation that does not change the Hamiltonian of the system. They differ just by the value of $\psi_h(\psi_t^0, u)$ on the helical axis, which ensures that ψ_H, ψ_{Ht} and ψ_{Hp} vanish there:

$$\psi_H = \psi_h(\psi_t^0, u) - \psi_h|_O, \tag{3.11}$$

where $\psi_h|_O = \psi_h(\psi_t^0, u)|_O$, whereas $\psi_H|_O = 0$. Equation (3.11), together with (3.1) and (3.2) for S_O and S_X, permits the interpretation of Φ_{OX} (which is the magnetic flux through the ribbon given by the O- and X-point orbits, as depicted in figure 1) as the helical flux through the separatrix surface. In fact,

$$-S_O = \psi_h|_O, \tag{3.12}$$

$$-S_X = \psi_h|_X = \psi_h|_O + \psi_H|_X, \tag{3.13}$$

simply yield

$$\Phi_{OX} = S_O - S_X = -\psi_H|_X. \tag{3.14}$$

Note that these considerations also apply to the next section.

https://doi.org/10.1017/S0022377824000941 Published online by Cambridge University Press

4. Magnetic islands as stand-alone domains

Magnetic islands, even if embedded in a global toroidal magnetic field, can be regarded as separated plasma domains. In a previous work (Predebon *et al.* 2018), we described a method to characterize geometrically every isolated domain from discretized field maps. These maps are usually the outcome of a field-line tracing code or an MHD code: starting from a set of points in the usual cylindrical coordinates (R, Z, φ) – with R the distance from the axis of the torus, Z the distance from the equatorial plane and φ the geometrical toroidal angle – the method allows to obtain a magnetic coordinate system $(\psi_{It}, \vartheta_I, \varphi)$ in the island, with the following expression for the magnetic field $\boldsymbol{B}$:

$$\boldsymbol{B} = \frac{1}{2\pi}(\nabla\psi_{It} \times \nabla\vartheta_I + \iota_I(\psi_{It})\nabla\varphi \times \nabla\psi_{It}), \tag{4.1}$$

where $\iota_I(\psi_{It}) = \mathrm{d}\psi_{Ip}/\mathrm{d}\psi_{It}$ is the rotational transform inside the island, φ the toroidal angle and ϑ_I the poloidal angle such that the field lines are straight on the (ϑ_I, φ) plane, with $d\vartheta_I/d\varphi = \iota_I(\psi_{It})$. As φ is the geometric toroidal angle, these coordinates are called symmetry flux coordinates (D'haeseleer *et al.* 1991). We remark that the $(\psi_{It}, \vartheta_I, \varphi)$ and $(\psi_{Ht}, \vartheta_H, \varphi)$ systems, being flux coordinates sharing the same toroidal angle, are mathematically equivalent. The indexes $\cdot_I$ and $\cdot_H$ denote the different procedure used to generate the respective flux coordinate systems.

Due to the high curvature of the surfaces in the proximity of the X-point, the method developed by Predebon *et al.* (2018) does not allow to get an accurate description of the geometry in that region, thus we limit our reconstruction to the surface immediately preceding the separatrix. This is assumed to be the boundary of our domain.

There is freedom in the choice of the radial coordinate. Once a normalized radial coordinate ρ_I is defined such that $\rho_I = 0$ on the magnetic axis and $\rho_I = 1$ on the last closed magnetic surface of the domain, and the Jacobian matrix $\mathrm{d}(R, Z, \varphi)/\mathrm{d}(\rho_I, \vartheta_I, \varphi)$, or equivalently $\mathrm{d}(x, y, z)/\mathrm{d}(\rho_I, \vartheta_I, \varphi)$, is known, we can calculate the (inverse) metric tensor $g^{ij} = \nabla x^i \cdot \nabla x^j$ and the Jacobian $J = \sqrt{g}$, which for the coordinates $(\rho_I, \vartheta_I, \varphi)$ will be explicitly written as J_I.

As the metric tensor is well defined in the whole island domain, we introduce here the observables that we intend to compare with the other approaches. Let us consider the width of the island itself. This can be measured with the ruler or can be calculated using the metric tensor. At a given toroidal angle $\varphi = \bar{\varphi}$, for a fixed poloidal angle $\vartheta_I = \bar{\vartheta}_I$, the (curvilinear) distance covered along the ρ_I direction from the magnetic axis to a generic surface with $\rho_I \leq 1$ is

$$L|_{(\bar{\vartheta}_I, \bar{\varphi})}(\rho_I) = \int_0^{\rho_I} g^{1/2}_{\rho_I\rho_I}(\rho_I', \bar{\vartheta}_I, \bar{\varphi})\,\mathrm{d}\rho_I', \tag{4.2}$$

where we have used the infinitesimal line element expression $\mathrm{d}l^2 = g_{ij}\,\mathrm{d}x^i\,\mathrm{d}x^j$ restricted to the radial direction. In figure 3, we show the $\varphi = 0$ section of a (1, 1) island in a circular tokamak based on the RFX-mod geometry, obtained again with the field line tracing code Flit. At this section, the $\vartheta_I = 0$ and $\vartheta_I = \pi$ coordinate lines correspond to the horizontal cut of the island, so that the island width is simply given by

$$W_I|_{\bar{\varphi}=0} = L|_{(0,0)}(1) + L|_{(\pi,0)}(1). \tag{4.3}$$

Other useful quantities for a comparison with the other approaches include the volume enclosed by the surface with radius ρ_I,

$$V_I(\rho_I) = \int_{[0,\rho_I]\times[0,2\pi]\times[0,2\pi]} J_I\,\mathrm{d}\rho_I'\,\mathrm{d}\vartheta_I\,\mathrm{d}\varphi, \tag{4.4}$$

https://doi.org/10.1017/S0022377824000941 Published online by Cambridge University Press

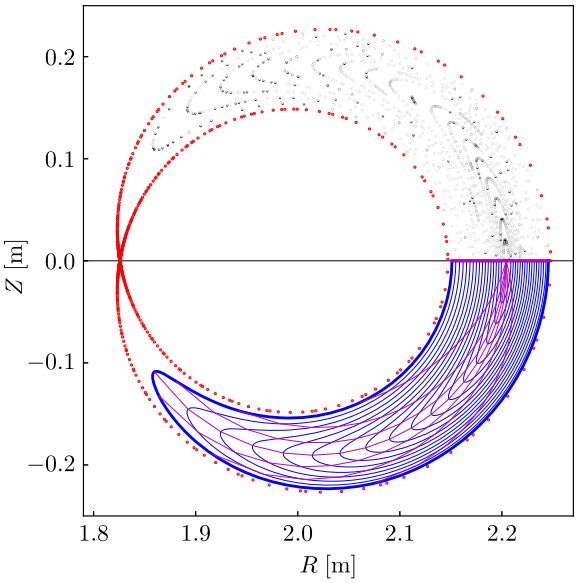

FIGURE 3. $\varphi = 0$ discretized field map of a (1,1) island in a circular tokamak (top half of the section) and corresponding flux-coordinate grid (bottom half) with the $\rho_I = \text{const.}$ lines (in blue, thick for $\rho_I = 1$) and the $\vartheta_I = k\pi/8$, k integer lines (in purple, thick for $\vartheta_I = 0, \pi$).

as well as the poloidal (the ribbon poloidal flux, as it is called by D'haeseleer *et al.* (1991)) flux,

$$\psi_{Ip}(\rho_I) = \frac{1}{2\pi} \int_{[0,\rho_I]\times[0,2\pi]\times[0,2\pi]} B^{\vartheta_I} J_I \, \mathrm{d}\rho_I' \, \mathrm{d}\vartheta_I \, \mathrm{d}\varphi, \tag{4.5}$$

and the toroidal flux,

$$\psi_{It}(\rho_I) = \frac{1}{2\pi} \int_{[0,\rho_I]\times[0,2\pi]\times[0,2\pi]} B^{\varphi} J_I \, \mathrm{d}\rho_I' \, \mathrm{d}\vartheta_I \, \mathrm{d}\varphi, \tag{4.6}$$

where the poloidal and toroidal contravariant components of the field are given by $B^{\vartheta_I} = \boldsymbol{B} \cdot \nabla \vartheta_I$ and $B^{\varphi} = \boldsymbol{B} \cdot \nabla \varphi$, respectively.

Combining (4.5) and (4.6) to define the helical flux $\psi_{IH} = m\psi_{Ip} - n\psi_{It}$, the island width can be again inferred from (2.11) with $\Phi_{OX} = -\psi_{IH}|_X$, as in (3.14), since the helical flux on the island axis vanishes identically. In this case, the Φ_{OX} flux is calculated at $\rho_I = 1$, not at the separatrix, as a line integral following one of the tips of the island, which is the curve that best approximates the separatrix, corresponding to the angle $u_I = m\vartheta_I - n\varphi = \pm\pi/2$.

5. A comparison of the different approaches

In the following, we provide a comparison of some observables using the different approaches described above. For this comparison, we consider the islands already introduced in the previous sections, namely a (1,1) island in a circular tokamak and a (1,7) island in the RFP, both based on RFX-mod, a circular toroidal device with major radius $R_0 = 2$ m and minor radius $a = 0.46$ m which can perform operation in either configuration (Sonato *et al.* 2003).

The reconstruction of the magnetic island topology is based on the calculation of the helical perturbations to the zeroth-order equilibrium. According to the procedure

https://doi.org/10.1017/S0022377824000941 Published online by Cambridge University Press

developed by Zanca & Terranova (2004), this is done solving a Newcomb-like equation, i.e. the linearized force-balance equation with the linearized Ampere's law ensuring a divergence-free magnetic field, using the external magnetic measurements as boundary conditions. Due to the set of measurements available in RFX-mod (48 toroidal arrays of four poloidally equispaced probes for both the radial and toroidal field components), a rich spectrum of Fourier components can be reconstructed for the magnetic perturbations. In this work, we focus on the dominant resonant Fourier component generating the (m, n) island, as specified in (2.3) and (2.4). The mode is $(m, n) = (1, 1)$ for the tokamak case, pulse 38 818 at $t = 362$ ms and $(m, n) = (1, 7)$ for the RFP case, which is the averaged discharge described by Momo *et al.* (2020). The resulting islands have been characterized geometrically by Predebon *et al.* (2018), where the discretized field maps have been produced by the field line tracing code Flit (Innocente *et al.* 2017) which is indeed based on Newcomb's perturbed fluxes as input.

As already mentioned, the comparison with the stand-alone approach of § 4 is possible only within the surface $\rho_I = 1$, which for both the RFP and tokamak islands is the last surface of the Poincaré section before the separatrix. For the other approaches, the radial domain extends from the O-point of the island to the separatrix.

In figure 4 and table 1, we summarize the results of the comparison. In the figure, the toroidal flux, the rotational transform and the volume profiles are plotted as a function of the poloidal flux for the approaches of § 3 (red lines) and § 4 (black). In particular, the poloidal and toroidal fluxes and the rotational transform defining the island flux surfaces are computed from (3.5) and (3.10) in the approach of § 3, and from (4.5) and (4.6) in the approach of § 4. The volume is computed in both cases from (4.4), using the related coordinate system and Jacobian. The comparison can be considered satisfactory. The small difference in the reconstruction of the rotational transform profile (approximately 0.4 % at the surface $\rho_I = 1$ for the tokamak, 0.5 % for the RFP) explains the pointwise differences in the fluxes that appear in the following table.

For the two islands, in the table, we review the most relevant quantities calculated at the X-point and at the last surface at the Poincaré map ($\rho_I = 1$). For the perturbative method of § 3 applied to the $\rho_I = 1$ surface, we assume $\psi_{Hp}|_{\rho_I=1} = \psi_{Ip}|_{\rho_I=1}$ and derive the other quantities based on this reference value. The island volume, and the toroidal and poloidal fluxes through the island are reported in the first block of the table. In the second block, the Φ_{OX} flux is computed from (2.10) for the approach of § 2, as the helical flux through the separatrix using (3.14) for the approach of § 3, and as the path integral along the (best approximation of the) X-point identified by the angle $u_I = m\vartheta_I - n\varphi = \pm\pi/2$ in the geometric approach of § 4 (proving also that $\Phi_{OX} = -S_X$ when the fluxes vanish on the O-point). Then, for the three methods, the related island width is calculated with (2.11). To complete the table, we also report the island width as resulting from (4.3) and as measured with a ruler from the Poincaré maps at $\varphi = 0$, $W_r|_{\bar{\varphi}=0}$.

The method which best estimates $W_r|_{\bar{\varphi}=0}$ is that of § 4, which is not surprising as the island geometry is directly derived from the Poincaré map itself: the $W_I|_{\bar{\varphi}=0}$ width from (4.3) perfectly matches $W_r|_{\bar{\varphi}=0}$. From the Φ_{OX} flux calculated as path integral along one of the tips of the island, we provide the width $W_{\Phi_{OX}}$ from (2.11), which yields a value within 1 % and 5 % error with respect to $W_r|_{\bar{\varphi}=0}$, for tokamak and RFP, respectively.

However, the perturbative methods of §§ 2 and 3 overestimate the total island width, within 6 % and 10 % error with respect to $W_r|_{\bar{\varphi}=0}$, for tokamak and RFP case, respectively. We recall that the formula of (2.11) for $W_{\Phi_{OX}}$ comes from the formal analogy between the typical textbook deformation of the flux surfaces around the resonance due to the opening of a magnetic island and the phase diagram of a pendulum, valid for small perturbations. This explains the error introduced by the application of this formula to the specific cases

https://doi.org/10.1017/S0022377824000941 Published online by Cambridge University Press

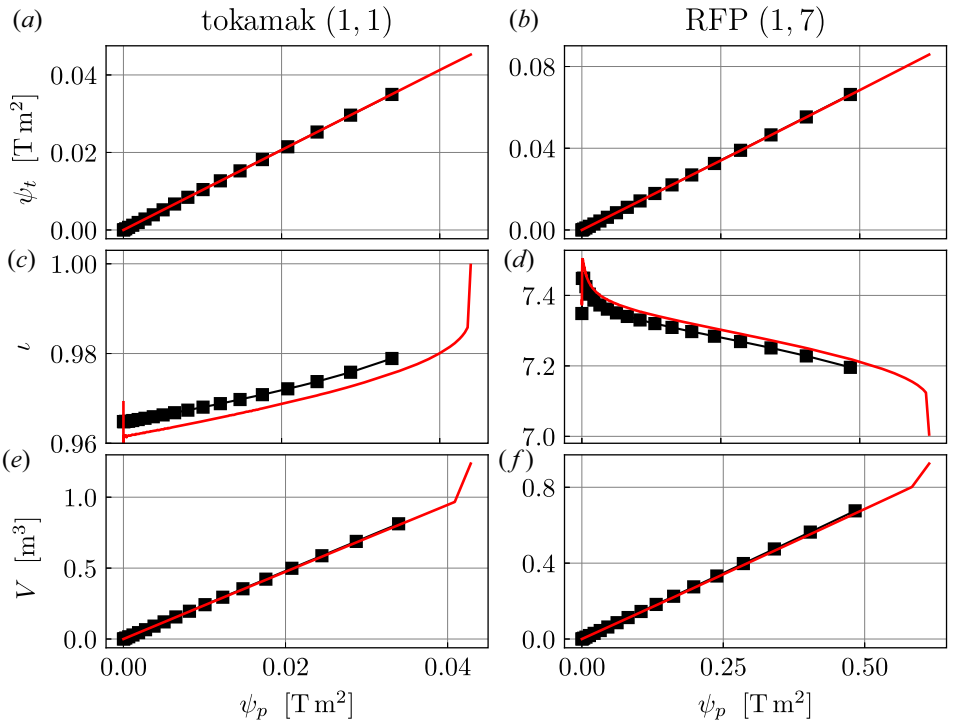

FIGURE 4. (*a*,*b*) Toroidal flux, (*c*,*d*) ι and (*e*,*f*) volume as a function of the poloidal flux for (*a*,*c*,*e*) a (1,1) tokamak island and (*b*,*d*,*f*) a (1,7) RFP island, for the approaches of § 3 (red lines) and § 4 (black).

Island	Surface	V_H [m^3]†	ψ_{Ht} [Tm^2]†	ψ_{Hp} [Tm^2]†	V_I [m^3]‡	ψ_{It} [Tm^2]‡	ψ_{Ip} [Tm^2]‡
tok (1, 1)	$\rho_I = 1$	0.806	3.49×10^{-2}	3.38×10^{-2}	0.813	3.50×10^{-2}	3.40×10^{-2}
	separ.	1.237	4.50×10^{-2}	4.39×10^{-2}	—	—	—
RFP (1, 7)	$\rho_I = 1$	0.673	6.61×10^{-2}	4.83×10^{-1}	0.676	6.63×10^{-2}	4.83×10^{-1}
	separ.	0.925	8.58×10^{-2}	6.25×10^{-1}	—	—	—
		Φ_{OX} [Tm^2]†	$W_{\Phi_{OX}}$ [cm]†	Φ_{OX} [Tm^2]‡	$W_{\Phi_{OX}}$ [cm]‡	Φ_{OX} [Tm^2]$^\circ$	$W_{\Phi_{OX}}$ [cm]$^\circ$
tok (1, 1)	$\rho_I = 1$	1.12×10^{-3}	9.96	1.02×10^{-3}	9.49	—	—
	separ.	1.34×10^{-3}	10.86	—	—	1.35×10^{-3}	10.93
RFP (1, 7)	$\rho_I = 1$	2.05×10^{-2}	12.01	1.90×10^{-2}	11.57	—	—
	separ.	2.40×10^{-2}	13.01	—	—	2.40×10^{-2}	13.12
		$W_I\|_{\bar\varphi=0}$ [cm]‡	$W_r\|_{\bar\varphi=0}$ [cm]				
tok (1, 1)	$\rho_I = 1$	9.45	9.45				
	separ.	—	10.07				
RFP (1, 7)	$\rho_I = 1$	10.99	10.97				
	separ.	—	11.86				

TABLE 1. For a (1,1) tokamak island and a (1,7) RFP island, $\cdot^\dagger$ quantities refer to the perturbative method of § 3, $\cdot^\ddagger$ quantities to the non-perturbative method of § 4, $\cdot^\circ$ quantities to the perturbative method of § 2; in the second row, $W_{\Phi_{OX}}$ is calculated from Φ_{OX} by means of (2.11) for the three different methods: ${\Phi_{OX}}^\dagger = m\psi_{Hp} - n\psi_{Ht}$, ${\Phi_{OX}}^\ddagger = m\psi_{Ip} - n\psi_{It}$, ${\Phi_{OX}}^\circ$ as defined in (2.10). $W_I|_{\bar\varphi=0}$ is the width as defined in (4.3). $W_r|_{\bar\varphi=0}$ is the width measured with the ruler at $\varphi = 0$.

https://doi.org/10.1017/S0022377824000941 Published online by Cambridge University Press

shown here, where the perturbation cannot be considered small. Large perturbations cause a displacement of the O-point and X-point from the rational surface where the radial derivatives are calculated. However, the correction to Φ_{OX} when calculated as the helical flux through the island separatrix (method of § 3), with respect to its estimate based on the axisymmetric equilibrium (method of § 2), slightly improves the evaluation of the width.

6. Summary

We have considered three different approaches for a geometric characterization of magnetic islands: (i) perturbative; (ii) perturbative but leading to the definition of a new single-helicity equilibrium; and (iii) non-perturbative based on the availability of a discretized field map.

In the first perturbative method, the island is described in a Hamiltonian context using the definition of action S_γ of a magnetic system. The novelty of this approach, first introduced by Escande & Momo (2024), is the definition of a coordinate-independent flux with a clear geometrical meaning – here named Φ_{OX} – related to the island width through (2.11). This formula, coming from the analogy between a textbook magnetic island and the cat's eye shape of the phase diagram of a pendulum, is very similar to the classical formulae for the island width (Hazeltine & Meiss 1992; Park *et al.* 2008), but with a new meaning of the flux that appears in all other formulations. The second method, developed by Martines *et al.* (2011) and Momo *et al.* (2011) for the RFP equilibrium and here extended to the tokamak configuration, starts from a perturbative approach that sums the zeroth-order equilibrium and the single resonant perturbation generating the island, then leads to the definition of a new single-helicity equilibrium using definitions specific to Hamiltonian mechanics. The third, non-perturbative method, is based on the availability of a discretized field map and defines the island domain through its geometrical definitions, as first developed by Predebon *et al.* (2018).

A detailed comparison has been carried out among the three methods applying them to two experimental islands of RFX-mod, both tokamak and RFP. We have provided an estimate of some observables showing that they are, in general, in good agreement with each other. As a novelty, moreover, we have extended the use of the expression (2.11) for the island width in a broader context than the perturbative approach in which it was first developed, thanks to a more comprehensive geometric interpretation of the Φ_{OX} flux. In particular, the Φ_{OX} flux, originally defined as the flux through the ribbon defined by the O- and X-point orbits, is identified as the helical flux through the island separatrix.

As a final remark, the (third) non-perturbative method, strictly based on the geometry of the flux surfaces, is the one which provides the most accurate description of the island observables for a large part of the island domain, failing, however, to describe the separatrix due to the high curvature of the flux surfaces in the neighbourhood of the X-point. This approach applies to any isolated region of the plasma, without any assumptions on the symmetry of the system and the possible interactions with other perturbations with different helicities. However, the two perturbative methods provide a geometric characterization which is in reasonable agreement with the non-perturbative method, at least in the cases with a strong helical symmetry. Easier to apply, based as they are on a single-mode perturbation from a linear Newcomb-like analysis, these methods can satisfactorily highlight the most relevant features of an island without the need to build discretized field maps and/or use MHD codes, providing a viable method for a fast description of a magnetic island domain.

https://doi.org/10.1017/S0022377824000941 Published online by Cambridge University Press

Acknowledgements

The authors are grateful to D.F. Escande and P. Zanca for reading the manuscript and providing useful observations.

Editor Nuno Loureiro thanks the referees for their advice in evaluating this article.

Funding

This research received no specific grant from any funding agency, commercial or not-for-profit sectors.

Declaration of interest

The authors report no conflict of interest.

REFERENCES

ARNOL'D, V.I. 2013 *Mathematical Methods of Classical Mechanics*, vol. 60. Springer Science & Business Media.

CARY, J.R. & LITTLEJOHN, R.G. 1983 Noncanonical Hamiltonian mechanics and its application to magnetic field line flow. *Ann. Phys. (N.Y.)* **151** (1), 1–34.

D'HAESELEER, W.D., HITCHON, W.N.G., CALLEN, J.D. & SHOHET, J.L. 1991 *Flux Coordinates and Magnetic Field Structure: A Guide to a Fundamental Tool of Plasma Theory*. Springer.

ELSASSER, K. 1986 Magnetic field line flow as a Hamiltonian problem. *Plasma Phys. Control. Fusion* **28** (12A), 1743.

ESCANDE, D. & MOMO, B. 2024 Description of magnetic field lines without arcana. *Rev. Mod. Plasma Phys*. **8** (16).

HAZELTINE, R.D. & MEISS, J.D. 1992 *Plasma Confinement*, 1st edn, vol. 86. Addison-Wesley.

INNOCENTE, P., LORENZINI, R., TERRANOVA, D. & ZANCA, P. 2017 FLiT: a field line trace code for magnetic confinement devices. *Plasma Phys. Control. Fusion* **59** (4), 045014.

MARTINES, E., LORENZINI, R., MOMO, B., TERRANOVA, D., ZANCA, P., ALFIER, A., BONOMO, F., CANTON, A., FASSINA, A., FRANZ, P. & INNOCENTE, P. 2011 Equilibrium reconstruction for single helical axis reversed field pinch plasmas. *Plasma Phys. Control. Fusion* **53**, 035015.

MOMO, B., ISLIKER, H., CAVAZZANA, R., ZUIN, M., CORDARO, L., BRUNA, D.L., MARTINES, E., PREDEBON, I., REA, C., SPOLAORE, M., VLAHOS, L. & ZANCA, P. 2020 The phenomenology of reconnection events in the reversed field pinch. *Nucl. Fusion* **60**, 056023.

MOMO, B., MARTINES, E., ESCANDE, D. & GOBBIN, M. 2011 Magnetic coordinate systems for helical SHAx states in reversed field pinch plasmas. *Plasma Phys. Control. Fusion* **53**, 125004.

PARK, J., BOOZER, A.H. & MENARD, J.E. 2008 Spectral asymmetry due to magnetic coordinates. *Phys. Plasmas* **15** (6), 064501.

PINA, E. & ORTIZ, T. 1988 On Hamiltonian formulations of magnetic field line equations. *J. Phys. A: Math. Gen*. **21** (5), 1293.

PREDEBON, I., MOMO, B., SUZUKI, Y. & AURIEMMA, F. 2018 Reconstruction of flux coordinates from discretized magnetic field maps. *Plasma Phys. Control. Fusion* **60** (4), 045003.

PREDEBON, I., MOMO, B., TERRANOVA, D. & INNOCENTE, P. 2016 MHD spectra and coordinate transformations in toroidal systems. *Phys. Plasmas* **23** (9), 092508.

SONATO, P., CHITARIN, G., ZACCARIA, P., GNESOTTO, F., ORTOLANI, S., BUFFA, A., BAGATIN, M., BAKER, W., DAL BELLO, S., FIORENTIN, P., GRANDO, L., MARCHIORI, G., MARCUZZI, D., MASIELLO, A., PERUZZO, S., POMARO, N. & SERIANNI, G. 2003 Machine modification for active MHD control in RFX. *Fusion Engng Des*. **66–68**, 161–168.

WHITE, R.B. 2013 *The Theory of Toroidally Confined Plasmas*, 3rd edn. World Scientific Publishing Company.

ZANCA, P. & TERRANOVA, D. 2004 Reconstruction of the magnetic perturbation in a toroidal reversed field pinch. *Plasma Phys. Control. Fusion* **46**, 1115–1141.